

# Clinical PET/MRI in neurooncology: opportunities and challenges from a single-institution perspective

Lisbeth Marner<sup>1</sup> · Otto M. Henriksen<sup>1</sup> · Michael Lundemann<sup>2</sup> · Vibeke André Larsen<sup>3</sup> · Ian Law<sup>1</sup>

Received: 18 September 2016 / Accepted: 31 October 2016 / Published online: 18 November 2016  
© Italian Association of Nuclear Medicine and Molecular Imaging 2016

## Abstract

**Purpose** Magnetic resonance imaging (MRI) plays a key role in neurooncology, i.e., for diagnosis, treatment evaluation and detection of recurrence. However, standard MRI cannot always separate malignant tissue from other pathologies or treatment-induced changes. Advanced MRI techniques such as diffusion-weighted imaging, perfusion imaging and spectroscopy show promising results in discriminating malignant from benign lesions. Further, supplemental imaging with amino acid positron emission tomography (PET) has been shown to increase accuracy significantly and is used routinely at an increasing number of sites. Several centers are now implementing hybrid PET/MRI systems allowing for multiparametric imaging, combining conventional MRI with advanced MRI and amino acid PET imaging. Neurooncology is an obvious focus area for PET/MR imaging.

**Methods** Based on the literature and our experience from more than 300 PET/MRI examinations of brain tumors with <sup>18</sup>F-fluoro-ethyl-tyrosine, the clinical use of PET/MRI in adult and pediatric neurooncology is critically reviewed.

**Results** Although the results are increasingly promising, the added value and range of indications for multiparametric imaging with PET/MRI are yet to be established.

Robust solutions to overcome the number of issues when using a PET/MRI scanner are being developed, which is promising for a more routine use in the future.

**Conclusions** In a clinical setting, a PET/MRI scan may increase accuracy in discriminating recurrence from treatment changes, although sequential same-day imaging on separate systems will often constitute a reliable and cost-effective alternative. Pediatric patients who require general anesthesia will benefit the most from simultaneous PET and MR imaging.

**Keywords** PET/MRI · FET · Brain tumor · Glioma · Pediatric · Multiparametric imaging · <sup>18</sup>F-fluoro-ethyl-tyrosine

## Abbreviations

AC	Attenuation correction
ADC	Apparent diffusion coefficient
BV	Blood volume
Cho	Choline
Cr	Creatine
CT	Computed tomography
DCE	Dynamic contrast enhanced
DSC	Dynamic susceptibility contrast
DTI	Diffusion tensor imaging
DWFS	Dixon water–fat separation
DWI	Diffusion-weighted imaging
EPI	Echoplanar imaging
FDG	<sup>18</sup> F-fluoro-deoxy-glucose
FDOPA	<sup>18</sup> F-fluoro-phenylalanine
FET	<sup>18</sup> F-fluoro-ethyl-tyrosine
MET	<sup>11</sup> C-Methionine
MRI	Magnetic resonance imaging
MRS	Magnetic resonance spectroscopy
NAA	<i>N</i> -Acetylaspartate

✉ Ian Law  
ilaw@dadlnet.dk

<sup>1</sup> Department of Clinical Physiology, Nuclear Medicine and PET, Copenhagen University Hospital Rigshospitalet, 9 Blegdamsvej, 2100 Copenhagen, Denmark

<sup>2</sup> Department of Oncology, Copenhagen University Hospital Rigshospitalet, 9 Blegdamsvej, 2100 Copenhagen, Denmark

<sup>3</sup> Department of Radiology, Copenhagen University Hospital Rigshospitalet, 9 Blegdamsvej, 2100 Copenhagen, Denmark

PET	Positron emission tomography
PWI	Perfusion-weighted imaging
TE	Echo time
$T_{\max}/B$	Maximum tumor to mean background uptake ratio
UTE	Ultrashort echo time

## Introduction

Imaging plays a key role in the management of patients with brain tumors at all stages of the disease: from the initial workup of patients with a suspected intracranial neoplasm, to planning of surgery and radiotherapy, and finally for detection of recurrent or progressive disease prompting changes of therapy. As histological confirmation may be difficult to obtain (or associated with considerable risk), one key requirement of imaging is to correctly separate malignant tissue from other pathologies and treatment-induced changes.

With its superior soft tissue characterization capabilities, magnetic resonance imaging (MRI) is the modality of choice in daily routine. However, standard anatomical MRI may not reliably predict the grade of malignancy or growth potential of a lesion. Furthermore, MRI interpretation becomes increasingly challenging after surgical trauma, radiation, and chemotherapy inducing necrosis with disruption of anatomical structures and increasing incidence of non-specific treatment induced signal changes caused by inflammation, edema, demyelination, ischemia, and metal implants. Novel treatment strategies, such as anti-angiogenic or immune therapy, may conceal or overexpress T1 contrast enhancement, thereby further compromising the diagnostic accuracy of response assessment [1, 2]. In radiotherapy-treated glioma patients, the specificity of standard MRI may be as low as 50% for detection of recurrent disease [3], and in non-enhancing tumors with MRI characteristics of low-grade glioma, 40% can be demonstrated to contain high-grade foci [4, 5]. Various functional imaging techniques depicting specific biological properties of the tissues have been introduced to complement standard MRI including both advanced MRI techniques [6] and positron emission tomography (PET) [7, 8]. Individually, these techniques have been reported to improve the diagnostic accuracy of standard MRI, and combining PET and advanced MRI could potentially further improve the overall diagnostic accuracy and in turn patient management.

An increasing number of institutions are implementing a hybrid PET/MRI scanner to supplement the use of PET/CT (computed tomography). The role of  $^{18}\text{F}$ -fluorodeoxy-glucose (FDG) PET/CT in oncology is well-established as an accessible, fast and accurate clinical tool

for whole-body cancer staging, monitoring and treatment planning. In contrast, the clinical role for combined PET/MRI scanners first introduced in 2008 [9] is still to be defined. Neurooncology appears to be an obvious application of clinical PET/MRI, and several recent reviews have highlighted the potential of multiparametric imaging of brain tumors [10–13], although the number of published studies actually exploring the potentials of hybrid PET/MR in neurooncology is limited [14–17]. These reviews will not be repeated; rather this paper is a critical appraisal of the clinical use of PET/MRI in neurooncology based on our single-institution experiences over the past 4 years focusing on gliomas. Using our Siemens mMR system, we have performed more than 300 FET PET/MRI scans in research and clinical routine in adult and pediatric neurooncology.

## Imaging methods

### PET tracers

While the value of FDG PET for brain tumors is limited due to the high physiological uptake in normal gray matter, the evidence for the use of amino acid PET tracers targeting the L-amino acid transporter systems 1 and 2 in neurooncology is increasing [7, 8], and the number of sites using either  $^{11}\text{C}$ -methionine (MET),  $^{18}\text{F}$ -fluoro-ethyl-tyrosine (FET) or  $^{18}\text{F}$ -fluoro-phenylalanine (FDOPA) on a regular basis is now substantial. Brain tumor imaging with these tracers has been shown to be rather similar [18–23], but only for MET [24] and FET [25] biopsy-verified thresholds of tumor uptake relative to background have been established to delineate the tumor extent of untreated gliomas.

A range of advanced MRI techniques show promising results from several studies. The techniques have been under development for the past 20 years, but are only slowly emerging into the clinic and are not sufficiently mature to be integrated into the recent standardized MRI protocol consensus recommendations for clinical trials in brain tumors [26]. Amino acid PET is superior to FDG and advanced MRI techniques [8], but due to the often challenging clinical situation it does not always point to the diagnosis.

Although a large cohort of consecutive patients ( $n = 124$ ) with MRI signs of recurrence or tumor progression of gliomas of mixed grades and histology showed an impressive diagnostic accuracy up to 95% for diagnosing active tumor using FET PET [27], this was dependent on the performance of a 60 min dynamic study. The diagnostic accuracy of a static 20 min PET acquisition was, however, only 71–75% depending on the metric compared

to 86–100% in previous studies [3, 28–30]. In a clinical PET/MRI setting, prolonged acquisition periods is preferably avoided to increase the work flow and patient comfort and decrease movement artifacts.

Although consensus guidelines are still to be established on the optimal techniques and implementations, the addition of advanced MRI sequences in a PET/MRI work flow is obvious. Firstly, the patients are typically referred to PET/MRI instead of MRI alone due to difficulties in separating malignant from benign lesions, and advanced MRI sequences may increase the diagnostic accuracy in this patient group. Secondly, the standard 20–40 min PET acquisition for FET typically leaves time for additional MRI sequences. An example of a comprehensive 40 min combined PET/MR evaluation is shown in Fig. 1. Finally, a combined acquisition facilitates comparison of the value of each modality when acquiring multiple modalities in the same space. In rare cases, multitracer PET imaging with a combination of, e.g., FET and FDG data (Fig. 2) may be applied, and acquisition with a PET/MRI scanner for one of the tracers will diminish the number of repeated scanning procedures for the patient.

In the following sections, general considerations of the basic and advanced MRI applied at our PET/MRI system in clinical and research brain tumor imaging protocols will be addressed, as well as the potential added value extrapolated from single-modality studies.

## MRI

The basic minimal anatomical MRI protocol for brain tumor imaging includes axial fluid-attenuated inversion recovery (FLAIR) and T2-weighted sequences visualizing non-enhancing tumor components, edema and therapy-induced gliosis, as well as a high-resolution isotropic 3D contrast-enhanced T1-weighted acquisition which depicts contrast leakage from the tumor vessels [2, 31].

Recently, it was suggested that brain tumor imaging in clinical trials should also include a pre-contrast 3D T1-weighted acquisition and axial diffusion-weighted imaging (DWI) [26]. Pre- and post-contrast T1-weighted imaging with identical sequence parameters allow for the creation of subtraction images, which has been proposed as a more accurate assessment of the contrast-enhancing tumor

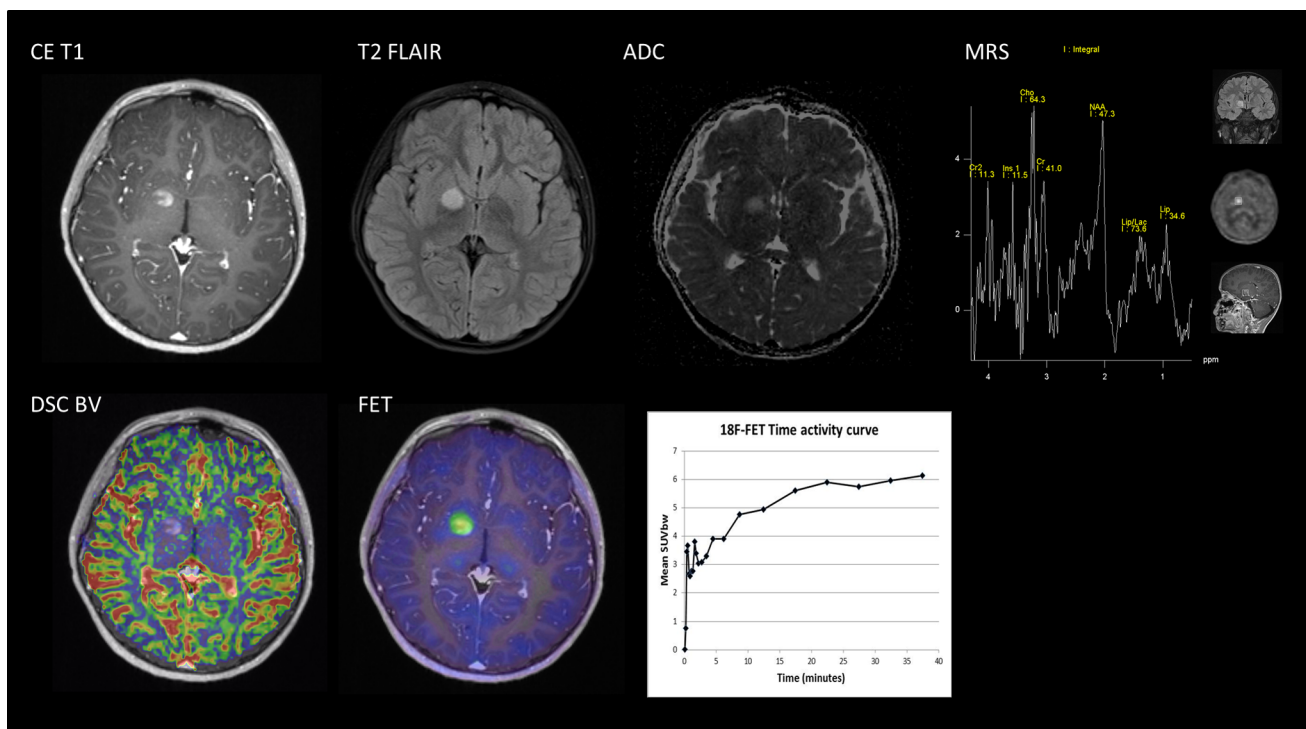


**Fig. 1** Multimodality tumor characterization. A combined 40 min dynamic FET PET/MRI with DSC BV and single voxel MRS was performed in a 7-year-old boy with an incidentally found lesion in the right basal ganglia area. Post-contrast T1 (CE T1) and T2 FLAIR show a solitary contrast-enhancing lesion without edema. Supplementary imaging included: DWI showing high ADC and thus not indicative of increased cellularity; MRS (short echo time) demonstrating only moderately increased choline (Cho/NAA = 1.36 and

Cho/Cr = 1.23); leakage-corrected DSC BV did not show increased BV; dynamic FET PET scanning found moderately increased uptake ( $T_{max}/B = 2.1$ ) with an increasing time–activity curve. Based on the combined imaging, a differentiation of a neoplasm from inflammatory (or other non-neoplastic) pathology could not be made, but it was concluded that a high-grade glioma or other aggressive malignancy was unlikely. Follow-up MRI after 3 months showed regression of contrast enhancement pointing toward a demyelinating lesion

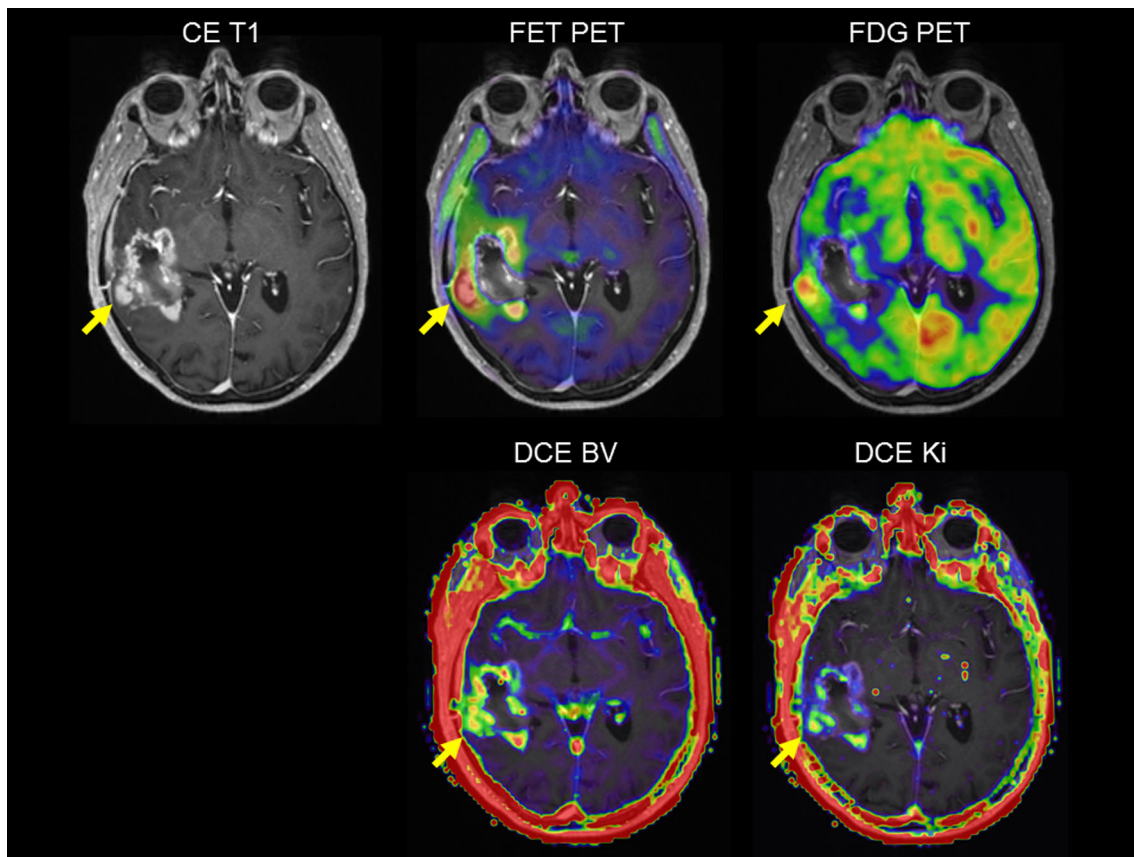


**Fig. 2** Multiparametric PET/MRI imaging. Transaxial images of glioblastoma (WHO IV) patient 2–3 weeks after surgery showing post-contrast MRI (CE T1), FET PET and FDG PET (top row), and blood volume (BV) and permeability (Ki) maps derived from dynamic contrast-enhanced (DCE) T1 MRI scans [48]. DCE allows for the separation of contrast enhancement in a blood volume (BV)

and permeability (Ki) component. The physiological measures highlight different and complementary tumor characteristics. FET PET shows a superior contrast to healthy brain in delineating the tumor borders, and peak areas (yellow arrow) are not overlapping in metabolic and vascular physiological measures. FDG PET is challenged by high uptake in functioning neural tissue

volume and may be helpful to distinguish blood products and microbleeds from cancerous tissues, especially in the presence of anti-angiogenic therapy [6, 32]. The clinical value of T1 subtraction imaging remains to be established and is generally not included in clinical imaging protocols.

### Diffusion-weighted imaging

The apparent diffusion coefficient (ADC) from DWI is related to the water motility, and thus the tissue microenvironment, and may be used to identify tumor areas with high cellularity (with low ADC) or areas of edema (with high ADC). The ADC is calculated by acquiring a number of sequences with different diffusion weighting, measured by the  $b$ -value, in at least three different directions. As a minimum, it is recommended to obtain images with no diffusion weighting ( $b = 0 \text{ s/mm}^2$ ) and images of moderate diffusion weighting ( $b = 1000 \text{ s/mm}^2$ ). Optimally, the protocol should also include images with intermediate  $b$ -value, e.g.,  $b = 500 \text{ s/mm}^2$  [26].

Early changes in ADC have been associated with treatment outcome [33]. Moffat et al. [34] showed that patients characterized as responding to therapy had an increase in ADC (i.e., decreased cellularity) 3 weeks into therapy relative to pre-treatment. In contrast, the ADC of patients with progressive disease tended to remain stable. Likewise, changes in ADC have been shown to be a strong imaging biomarker in patients with GBM treated with bevacizumab [35, 36]. Reduced ADC may also be used to assess tumor grade in both children [37] and adults [38, 39] (Fig. 1).

By increasing the number of diffusion-encoding directions, typically to 20 or more (at the cost of increased acquisition time), it is possible to estimate a diffusion tensor at each image voxel, known as diffusion tensor imaging (DTI). Subsequent modeling makes it possible to infer the direction of diffusive processes and to estimate white matter fiber tracts (tractography), which can be valuable in pre-surgical planning [40] (Fig. 3).

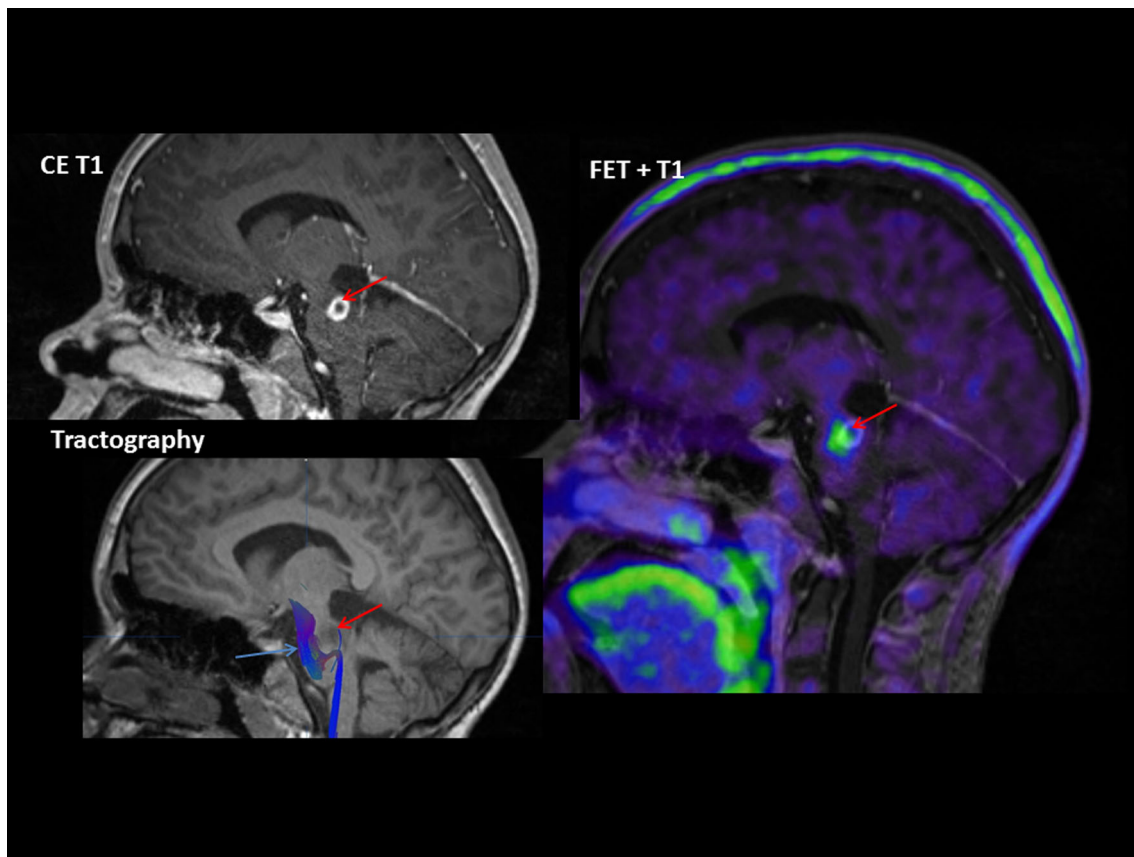


**Fig. 3** Presurgical planning. Sagittal images of a 15-year-old boy with pilocytic astrocytoma (WHO I). Post-contrast T1 MRI (*upper left*) showed contrast-enhancing tumor (*red arrow*) with high metabolic activity on FET PET in the anterior parts of the tumor ( $T_{\max}/B = 2.7$ , biological tumor volume = 2 ml). Tractography from

diffusion tensor imaging coregistered to pre-contrast T1 MRI (*lower left*) showed a close relationship of the corticospinal tract (*blue arrow*) to the tumor (*red arrow*). Thus, chemotherapy was decided to be safer than surgery

Traditionally, DWI is based on a fast single-shot echo planar imaging (EPI) technique, which makes it possible to acquire images in 20–100 ms. At higher field strengths, the technique is prone to susceptibility artifacts, especially at tissue interfaces, around surgical cavities and metallic implants, which lead to geometrical distortions and signal dropout. Recently, a novel method using parallel imaging and readout-segmented EPI with non-linear phase correction (clinically available on Siemens hardware as RESOLVE DWI) has been proposed for high-resolution DWI with reduced susceptibility artifacts [41]. Standard DWI for assessment of tumor grade is used in daily clinical routine, but the role in the assessment of tumor recurrence and response evaluation has not been established.

### Perfusion-weighted imaging

Perfusion-weighted imaging (PWI) for mapping of tumor blood volume (BV) as a marker of tumor vascularization has been extensively studied in the past 25 years. Dynamic imaging is performed during the passage of an

intravenously administered bolus of a gadolinium-based MRI contrast agent. The original and most studied technique is dynamic susceptibility contrast (DSC) MRI based on T2\*-weighted imaging using a 2D EPI sequence (Figs. 1, 4 and 5). Alternatively, a 2D or 3D T1 sequence can be applied for dynamic contrast-enhanced (DCE) MRI (Fig. 2). By measuring the T2\* signal decrease (or increase using DCE), BV can be estimated as the area under the tissue concentration curve.

DSC BV imaging has been shown to be of value as a supplement to MRI for a range of clinical situations, in particular for tumor grading [42] and for differentiation of tumor progression from treatment-induced changes [43]. Standard analysis is based on visual reading and calculation of the relative BV by normalizing tumor BV to normal-appearing white matter in the contralateral hemisphere. Often, a cutoff of 1.75 derived in a study separating low- and high-grade gliomas is quoted [42], but reported optimal BV cutoffs for tumor grading and for separating progression from treatment-induced changes vary substantially between studies [43–45]. This variability

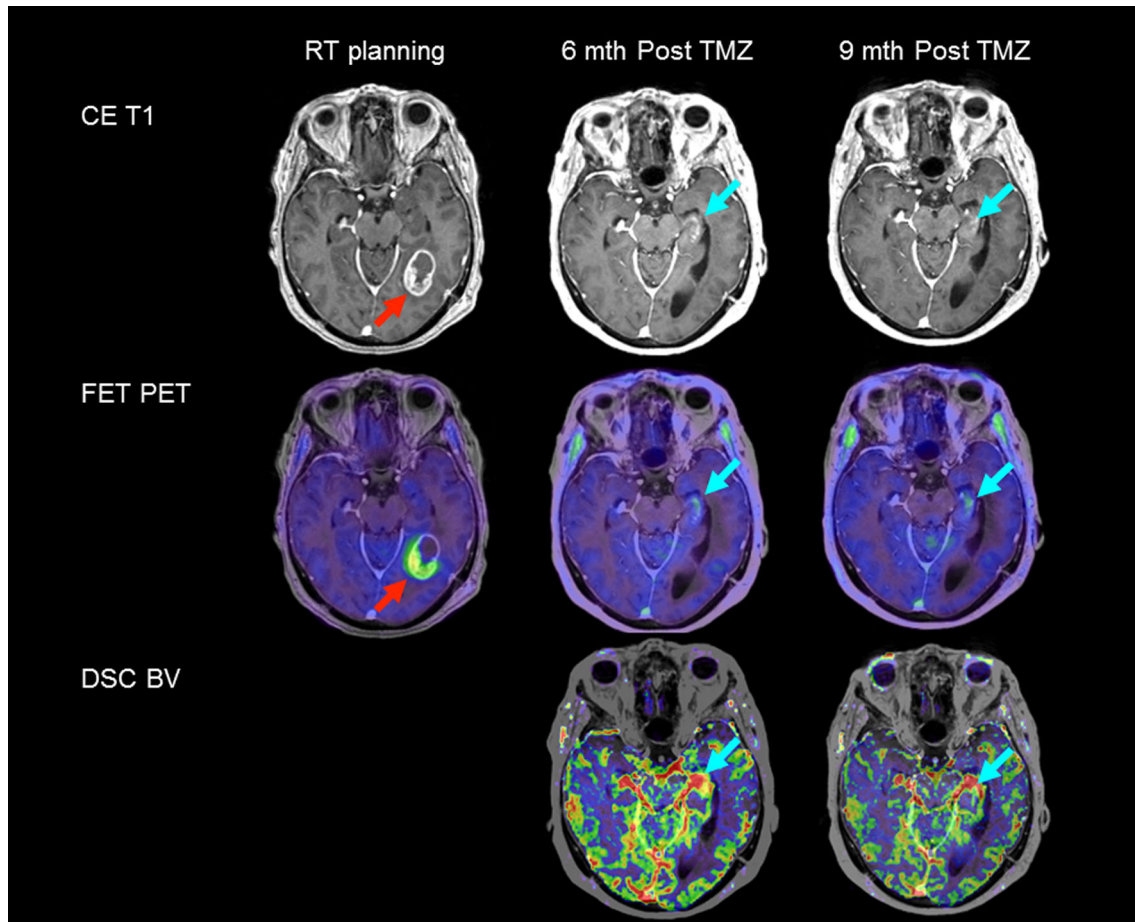


**Fig. 4** Tumor recurrence vs. treatment effects. Transaxial T1-weighted post-contrast MRI (*top row* CE T1), FET PET (*center row*) and leakage-corrected blood volume maps (*bottom row* DSC BV) in a patient with deep-seated glioblastoma multiforme (WHO IV) in the left inferior occipito-temporal lobe. The initial scans at radiotherapy planning (*left*) show 6 cm<sup>3</sup> of metabolically active tumor with FET uptake (*red arrow*,  $T_{\max}/B = 2.7$ ). Six months after termination of adjuvant temozolomide (TMZ), CE T1 MRI found increased contrast enhancement in the left hippocampus suspicious of

tumor recurrence, and the patient was scheduled for second-line chemotherapy. However, recurrence could not be corroborated by supplementary FET PET/MRI DSC scanning (*cyan arrow*,  $T_{\max}/B = 1.4$ ). Evidence of tumor angiogenesis could not be identified with certainty because of the high blood volume signal from surrounding vasculature and choroid plexus. Follow-up FET PET/MRI DSC after 3 months untreated showed stable conditions (*right column*) supporting treatment effects

probably reflects an overlap between normal and abnormal BV, and intra-lesion heterogeneity, but also the lack of consensus on how to perform and analyze DSC BV imaging. Recently, consensus recommendations have been published [46], but how to correct for contrast leakage in the presence of a disrupted blood–brain-barrier resulting in erroneous BV estimates is still not clear. In DSC, a pre-bolus or various post-processing leakage correction methods (or maybe preferably both) may be applied [47]. BV estimates are most accurate before resection and radiotherapy and may be challenged by treatment damage and metal implants. Figure 5 shows examples of DSC BV imaging in neurooncology as well as an example of the artifacts due to a metallic implant. In a PET/MRI study combining FET and DSC, we found that susceptibility

artifacts overlapped with MRI tumor volume and interfered with the interpretation in as many as 56% of cases [16].

Compared to DSC, the DCE approach offers several advantages: DCE (1) is less prone to artifacts due to metallic implants and air–bone interfaces, (2) does not suffer from image distortions facilitating image registration and (3) allows calculation of the actual concentration of the contrast agent, which in turn permits more elaborate kinetic modeling and absolute quantitation of BV and permeability (Fig. 2) [48]. However, most vendors and third party software solutions do not support DCE, and users usually rely on in-house software solutions limiting more widespread clinical use outside the research community.

Although increased BV is a well-established marker of malignancy at the group level, the clinical value of BV

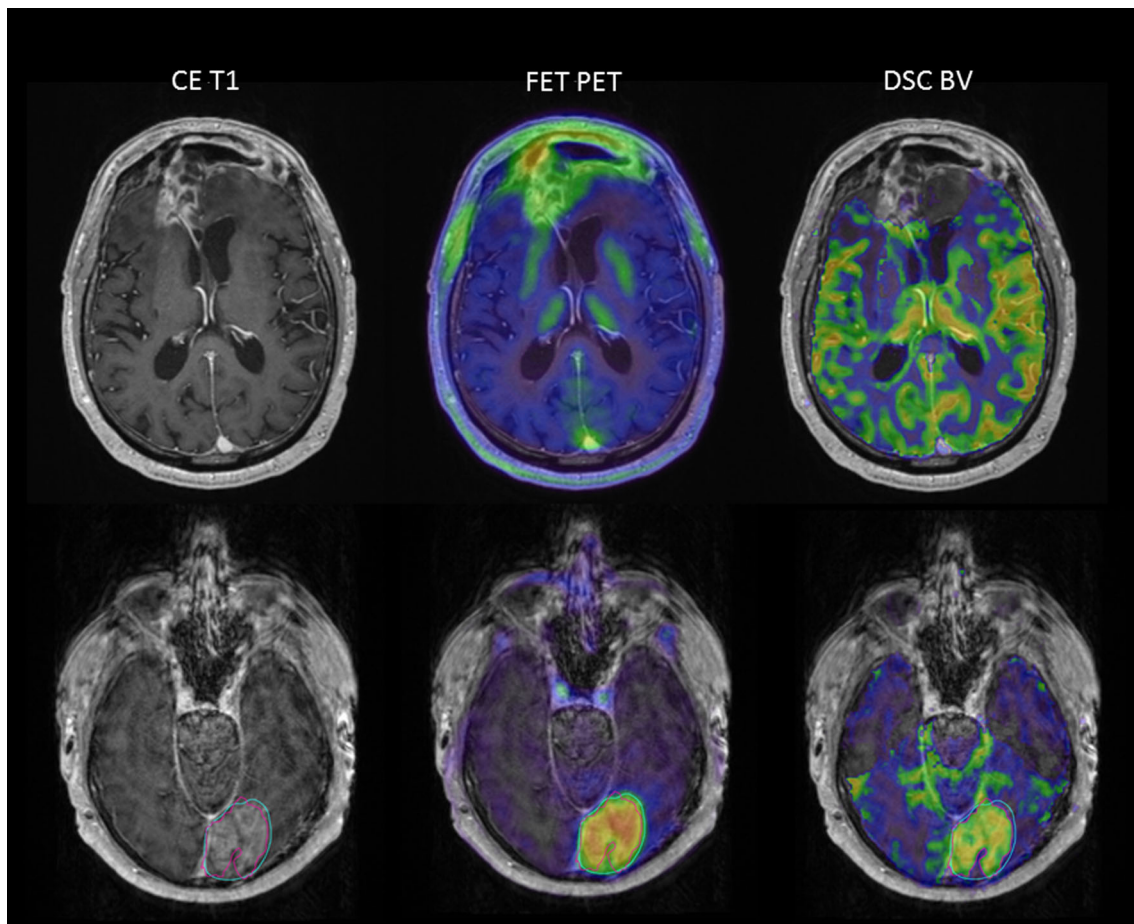


**Fig. 5** Limitations of multimodal imaging. Transaxial slices of contrast-enhanced T1 (CE T1), FET PET and DSC BV imaging, compromised by imaging artifacts. The patient in the upper row had prior surgery and radiotherapy for a sinonasal carcinoma and was referred to distinguish tumor recurrence from treatment effects. FET PET showed increased activity in the border of the lesions in the frontal region ( $T_{\max}/B = 3.2$ ) indicating recurrence, whereas blood

imaging at the single-patient level remains an area of continuing debate, both due to the lack of standardization of image acquisition and processing, and difficulties of interpretation related to the technical limitation of the DSC technique.

### Spectroscopy

A number of different metabolites relevant to the neuro-oncologic assessment can be visualized with magnetic resonance spectroscopy (MRS). The technique exploits that protons bound in various molecules behave slightly differently in a magnetic field due to different covalent electrons shielding the nucleus, which makes the metabolites resonate at slightly different frequencies. This small shift in frequency makes it possible to distinguish protons in various molecules. The area under each peak is proportional to the concentration of the corresponding

volume imaging (DSC BV) was not useful due to a severe susceptibility artifact induced by the inserted titanium net. The bottom row shows a patient with recurrent glioblastoma (WHO IV). Excellent agreement of blood volume imaging (DSC BV) and FET activity distribution is demonstrated, but CE T1 image quality is degraded due to pronounced patient motion. Often a 2D T1 sequence less sensitive to patient motion must be added

metabolite. At long echo times ( $TE > 130$  ms), the most prominent metabolites are *N*-acetylaspartate (NAA) related to normal functioning neuronal cells, choline (Cho) attributed to glial cell membrane turnover that correlates with the Ki67 proliferation marker [49] and creatine (Cr). Elevated Cho/NAA and Cho/Cr ratios have been shown to correlate with tumor grade [50] and to aid in distinguishing pseudo-progression from true tumor progression [51]. Reducing TE (to the order of 30 ms) makes it possible to detect other subtle metabolites. In pediatric neurooncology, reports suggest the possibility of discriminating between tumor types based on the spectroscopy metabolite profile [52], and it has been shown that the metabolite profile of recurrent brain tumor resembles the profile at diagnosis [53] (Fig. 1).

Although multivoxel MRS has been introduced, MRS is traditionally performed in a single voxel typically in the order of 1–6 mL, manually placed on the tumor border.

Positioning of the voxel is user dependent; however, with an integrated PET/MRI examination, one has the option of positioning the voxel based on the metabolic information from the PET acquisition, e.g., where the tracer uptake is maximum or in an area where the information from PET and other MR modalities are discordant, e.g., an area with high PET uptake, but with no contrast enhancement or high ADC.

A recent consensus statement concluded that MRS is “clinic ready for diagnostic, prognostic, and treatment assessment” of a variety of brain disorders including brain tumors [54]. However, meta-analyses have concluded that the diagnostic accuracy of MRS for tumor grading and separation of glioma recurrence from radiation necrosis is only moderate [55, 56]. The clinical value of spectroscopy for assessment of brain lesions at the single-patient level remains controversial, and the use in clinical routine probably reflects single-institution experiences. Currently, at our institution, clinical brain spectroscopy is limited to patients with metabolic disorders and is not included in clinical brain tumor MRI protocols.

### PET/MRI technical issues

Currently, clinical PET/MRI systems with simultaneous acquisition (as Siemens mMR and GE Signa scanners) are based on standard 3T MR systems fitted with an MR-compatible PET detector system. In terms of specifications, the PET and MRI systems are individually comparable to stand-alone systems, although the Siemens system is based on the older Magnetom Verio MR scanner and the PET system does not provide time-of-flight imaging.

### Attenuation correction

Lacking a transmission source, PET/MRI systems rely on MR images for attenuation correction (AC) of the PET acquisitions. Although often used, MRI-based approaches founded on segmentation of Dixon water–fat separation (DWFS) and the ultrashort echo time (UTE) sequences have been shown to be inaccurate for attenuation correction in the brain [57, 58]. Compared to CT-based AC, regional radiotracer activity concentrations obtained using DWFS and UTE are underestimated throughout the brain with a strong radial bias leading to an underestimation of the outer cortical regions and the cerebellum. Atlas-based method improves quantitation significantly [59, 60], but are based on patients represented in the atlas and may be difficult to apply in a neurooncology setting to patients with skull-deforming surgery or metallic implants, and in children. Consequently, the standardized semi-quantitative assessment of tumor extent and metabolism [61], which is one of

the main advantages of FET PET imaging, is erroneous. Although more recent AC developments in MRI-based methods are promising, e.g., RESOLUTE [62, 63], these need to be thoroughly evaluated using the standard clinical metrics for the individual tracer prior to routine clinical use (Fig. 6). At our center, we still rely on a separately obtained low-dose CT scan for AC for all brain PET/MRI scans [58].

### Movement artifacts

Head fixation equipment in the PET/MRI scanner is inferior to stand-alone MRI systems as attenuation of the PET signal using standard head fixation and earphones will reduce activity in the temporal areas in the reconstructed PET images [64]. Thus, movement artifacts constitute a larger problem in a PET/MRI scanner compared to stand-alone systems compromising both MRI (Fig. 5, lower row) and PET image quality (Fig. 7). We have applied a real-time head movement markerless tracking system (Tracoline, version 2, TracInnovations, Ballerup, Denmark) using infrared light. This allows for immediate repetition of MRI sequences with severe movements [65, 66], and preliminary and unpublished data suggest considerable image improvement of the PET scan when using the measured data for motion correction (Fig. 7).

### Multiparametric imaging

To date, only very few published studies have actually investigated the potential of combined amino acid PET and advanced MRI using hybrid systems. These studies have mainly focused on the feasibility and agreement of modalities [14, 16, 17] and less so on the diagnostic yield [15], but several mostly bi-modal studies have compared the information obtained from amino acid PET and MRI using separate systems.

BV and amino acid PET are the most common combination. Early comparative studies reported good spatial and quantitative agreement between DSC BV and amino acid PET [67, 68] (see Fig. 5, lower row) and of both with histological measures of malignancy [69]. More recent studies have confirmed a moderate quantitative correlation of BV and PET uptake, but have also demonstrated a poor spatial congruence in particular in low-grade [70] and treated gliomas (Fig. 2) [14, 16, 71]. Spatial incongruence may in part be related to less clear tumor delineation of BV imaging compared to PET (Fig. 4) [14, 71] and impaired tumor coverage due to susceptibility artifacts (Fig. 5) [16]. However, BV imaging and amino acid PET appear to provide



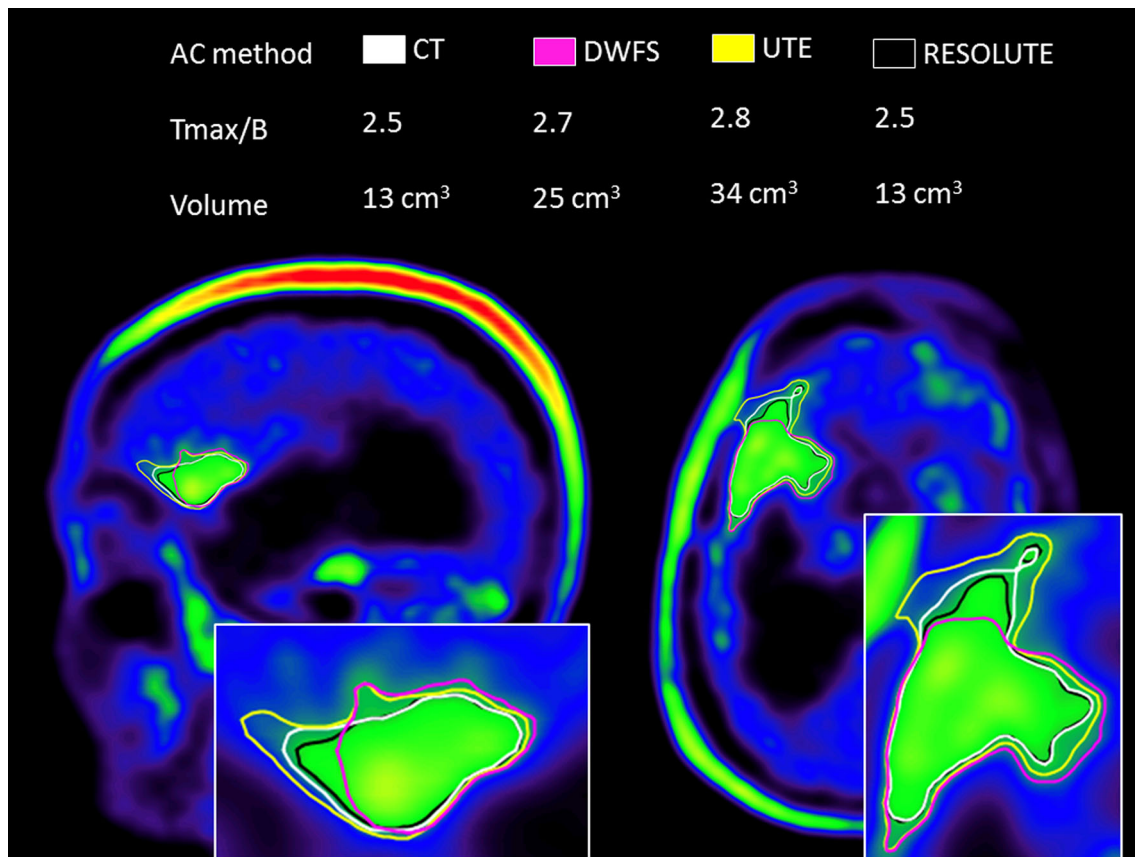


**Fig. 6** PET/MRI attenuation correction. Sagittal and axial image of simultaneous <sup>18</sup>F-FET PET/MRI acquisition of a 55-year-old female with anaplastic oligodendroglioma (WHO III) with the tumor borders delineated by activity >1.6 times the background in the healthy brain. The PET reconstruction is performed applying four different attenuation correction strategies using either CT (a low-dose CT performed on a separate PET/CT scanner), Dixon water–fat separation (DWFS),

ultrashort echo time (UTE) or RESOLUTE that identifies bone signal in the MRI. RESOLUTE (*white*) most accurately resembles CT attenuation correction (*black*) regarding both tumor volume and maximal tumor uptake relative to a background region ( $T_{\max}/B$ ). DWFS and UTE significantly overestimate volume and signal intensity and warp the configuration of the tumor due to radial error. The images were kindly provided by Claes Nøhr Ladefoged

complementary information on tumor biology and may be of value in particular in treated gliomas for separating tumor recurrence from tissue with treatment-induced changes or low growth potential (Fig. 4) [15, 16, 72].

MRS has been reported to supplement PET for characterizing intracerebral lesions [73, 74], biopsy planning (using multivoxel MRS) in PET-negative lesions [17, 75] and for detection of tumor recurrence [15, 76], but the findings are not entirely consistent as to whether the MRS improved sensitivity or specificity, and no general consensus on the choice of TE and voxel size exists.

Comparisons of PET and DWI for identifying areas of increased malignancy have provided conflicting results with some studies reporting good spatial agreement of PET hot spots and areas of reduced diffusivity [77, 78], and improved diagnostic accuracy when combining DWI and PET [79], while others have found poor spatial correlations [80–82] and little diagnostic value of adding DWI to PET [15, 70].

A few studies have investigated the diagnostic yield of a multiparametric approach using either hybrid PET/MRI or separate systems. Yoon [83] analyzed separately obtained FDG PET and both conventional and advanced MRI (ADC, DSC BV and MRS) for tumor grading in patients with untreated gliomas. Individually, the diagnostic accuracies of the functional imaging techniques were similar and combining any of them to conventional MRI improved positive predictive value from 90 to >95% and negative predictive value from 58% to between 63% (DWI) and 86% (FDG), depending on the combination. On adding a third parameter, the positive predictive value was >97% and negative predictive value  $\geq 80\%$  for all combinations (except DWI with 71%). Jena [15] investigated combined FET and advanced MRI (ADC, MRS, and DSC BV) in glioma patients with suspected recurrence. The accuracy of MRS (Cho/Cr) was highest and of ADC lowest. Combining FET, MRS and BV yielded the highest accuracy. It should be noted that only early FET imaging 0–25 min after

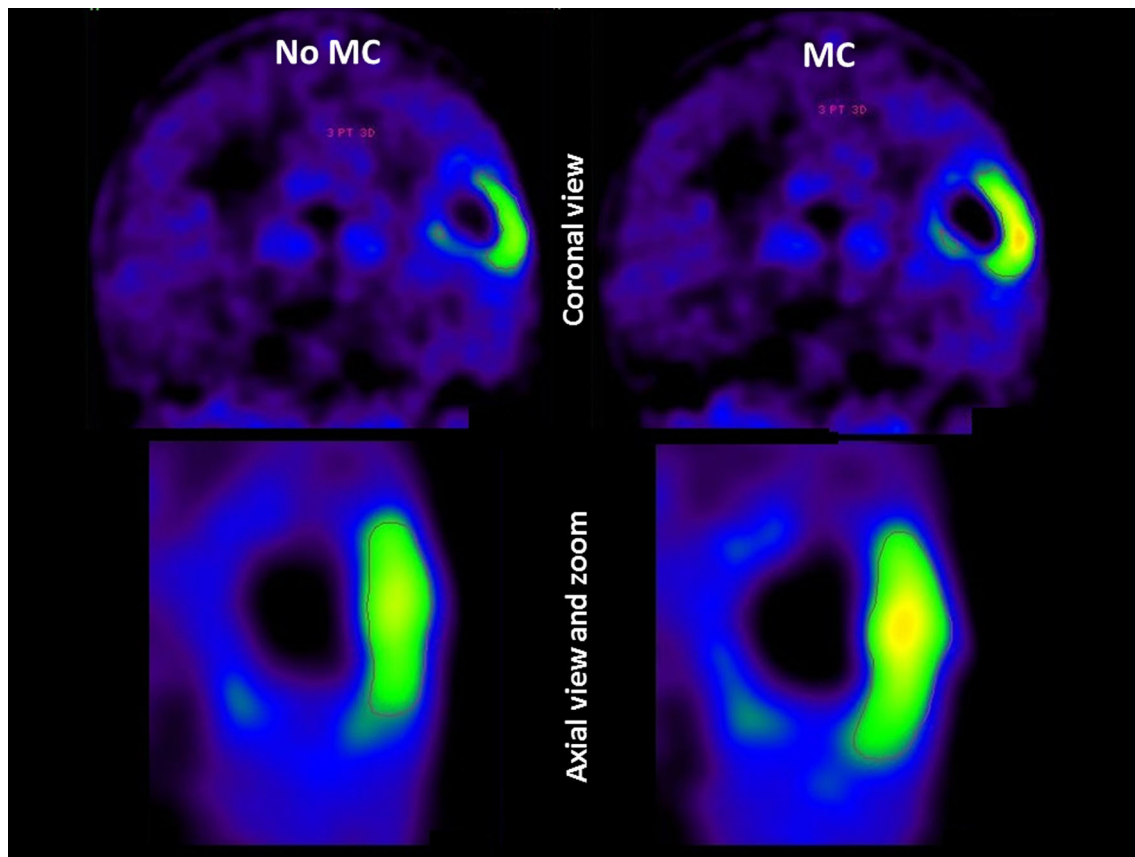


**Fig. 7** Motion correction of prolonged FET PET/MRI acquisitions. Coronal (*top*) and transaxial sections (*bottom*) of FET PET reconstructions from 20 to 40 min post-injection of a 9-year-old boy with giant cell glioblastoma (WHO IV). Markerless motion tracking (Tracoline, version 2) showed periodical head movements of 10–15 mm during the 40 min dynamic FET PET acquisition. Using

continuous tracking data, motion correction (MC) at a motion threshold of 5 mm was performed (*right side*), identifying and aligning a total of four subframes. In motion-corrected images,  $T_{\max}/B$  increased from 2.3 to 2.8 (19%) and the biological tumor volume increased from 7 to 11 cm<sup>3</sup>. Data were kindly provided by Andreas Ellegaard and Jakob Slipsager

injection was acquired, BV was performed without leakage correction and conventional MRI was not included in the analysis. D'Souza [84] compared MET and MRI including both MRS and DSC BV for evaluation of treatment response in high-grade glioma ( $n = 29$ ) treated with standard radio-chemotherapy. Diagnostic performance was not significantly different, but MET tended to be more sensitive (95 vs 84%) and less specific (80 vs 90%) compared to MRI including advanced techniques. Dunet [79] performed dynamic FET, MRI and both MRS (Cho/Cr) and DWI for grading of untreated gliomas. The accuracy of FET (67%) was slightly higher than histogram analysis of ADC maps (65%) and both markedly better than MRS (48%). Optimal sensitivity (86%) and specificity (100%) were obtained when combining ADC and FET.

Thus, there seem to be some literature support for increased accuracy or obtaining complementary information when combining conventional MRI, advanced MRI and PET. However, although various advanced MRI techniques have been available for more than two decades,

their diagnostic and clinical value in the neuroradiology community is not generally accepted and the incremental value of adding advanced MRI to amino acid PET may be even less evident.

### Clinical applications

Until now, PET in brain tumor imaging has been used primarily as a supplementary diagnostic aid performed after an equivocal routine MRI [8]. Simultaneous PET/MRI disrupts the sequential selection process. A more detailed analysis of selected patient groups or clinical questions that will benefit from both techniques is required, and a mere substitution of routine clinical MRI with FET PET/MRI cannot be recommended. Considering the increased radiation burden and costs, the added clinical value of routine PET would be disproportionately small.

The feasibility of PET/MRI for radiotherapy planning of meningioma has been demonstrated in two smaller studies using the somatostatin receptor II agonist <sup>68</sup>Ga-DOTATOC

[85, 86]. However, as a diagnostic CT of the head is always required for planning purposes, PET/MRI and separate CT does not provide any advantages compared to PET/CT and separate MRI, not least because of the AC issues in PET/MRI that could impact the delineation of the PET volume (Fig. 6).

In biopsy planning, most patients with a newly identified lesion will have a recent MRI available. Thus, in a large fraction of cases, repeating clinical MRI sequences in a PET/MRI session add little to understanding the condition of the patient.

We have considered that a combined amino acid PET/MRI is likely to improve the diagnostic accuracy of standard MRI in certain clinical situations dictated by the biological dynamics of the glioma:

1. Routine follow-up imaging is recommended in patients with high-grade gliomas after concomitant radio-chemotherapy in whom pseudo-progression (a toxic reaction developing after 1–6 months mimicking tumor progression on MRI [87]) or true tumor progression is suspected. These are common and clinically important conditions to recognize, as efficacious treatment may be substituted for second-line therapy or renewed surgical intervention [88], and combined imaging could accelerate decision making compared to a sequential imaging strategy.
2. In patients where both MRI and PET are equivocal in discriminating between tumor recurrence and treatment changes, a follow-up PET/MRI after 8–12 weeks will often resolve the issue.
3. Surveillance during chemotherapy of a low-grade glioma using PET/MRI may detect malignant transformation earlier [89].
4. PET/MRI at the first follow-up after initiating second-line chemotherapy, such as anti-angiogenic treatment, may allow early discrimination of responders from non-responders [90, 91].
5. Surveillance using PET/MRI during chemotherapy treatment pause (“drug holiday”) in high-grade glioma may detect recurrence earlier.

All the above situations, however, do not require simultaneous acquisition in a PET/MRI scanner, but can be solved by sequential imaging with MRI followed by PET scan on the same day for most patients. This has successfully been implemented at our institution. There are still a number of drawbacks using the combined PET/MRI scanner as compared to sequential imaging that need to be addressed:

1. PET/MRI is still a rather exclusive machinery and the present technical standard in the PET and MRI

components is not state of the art in all available systems.

2. The software solutions and the stability of the scanner are less robust as compared to stand-alone scanners and the clinical throughput of the combined scanner is significantly lower.
3. The aforementioned issues about attenuation correction affect the quantitative reliability and demands extra attention to the PET image.
4. The patient comfort is decreased when positioned in the narrower bore of the combined PET/MRI scanner, increasing the sensation of claustrophobia.
5. A rigid head fixation cannot be performed because of increased attenuation and only non-attenuating equipment should be used. Movement artifacts are thus more common in PET/MRI (Fig. 7) than in stand-alone scanners.
6. Earphones are still not standard equipment and thus the communication with the patient during the scan is hampered, decreasing the cooperation of the patients and image quality of the scan.

Thus, in our institution, neurooncology PET/MRI is prioritized for two indications: imaging research trials and pediatric neurooncology. In predictive biomarker imaging trials of new treatments to identify early responders, the reduced number of imaging procedures may be a significant factor in patient recruitment, simplifying the work flow and reducing costs for patient and neurooncologist.

This is particularly important in multitracer studies, i.e., an FDG PET/MRI in combination with an FET PET/CT (Fig. 2).

In pediatric neurooncology, there are additional factors to consider which make hybrid PET/MR an attractive technology in this group of patients:

1. The imaging environment is particularly unpleasant for the pediatric patient. Hybrid techniques should be prioritized to reduce this burden. Patients in the age of 0–6 years (and sometimes older) will require general anesthesia, and it may be considered unethical to perform two separate procedures if they can be combined into a single procedure.
2. The coregistration of separate FET PET and MRI is often challenged in children due to:
  - (a) the relatively larger field of view including high uptake areas of the mouth;
  - (b) differing head positioning strategies;
  - (c) the frequent location of pediatric tumors in the fossa posterior or medulla;
  - (d) high extracerebral FET uptake, e.g., in the bone marrow;

Coregistration issues can often be solved by removing images from the caudal field of view [92], but obtaining the scans in the same space in a PET/MRI scanner is superior.

3. When the tumor is located in the medulla oblongata or spinal cord, coregistration to MRI is challenged by the non-rigid position of the body and PET/MRI ensures correct alignment.

The clinical use of PET in pediatric neurooncology should be regarded as a research area. The literature is scarce, tumor histology is highly heterogeneous and often unusual, and evidence cannot be directly transferred from adult neurooncology that is dominated by gliomas. The literature of PET/MRI in pediatric neurooncology is limited to case reports and feasibility studies [93], but the prevailing literature does support a role for amino acid PET/MRI in pediatric neurooncology [73, 94–97].

Although PET/MRI thus appears to be the method of choice in pediatric neurooncology, its practical use is often difficult. The lengthy 90 min PET/MRI scan sessions when performing combined brain and spinal cord imaging may be stressful. Also, at our institution, the practical logistics of anesthesia has proven challenging and has limited access to imaging in younger children. The earlier-mentioned drawbacks using PET/MRI in adults also apply to children, and novel attenuation correction strategies need to be validated in the pediatric population separately taking the developing skull into account. Claustrophobia is more pronounced when using PET/MRI without earphones and isolated from comforting parents. Head movements are a problem in PET/MRI because of the longer acquisition times and the special demands for head fixation in children with smaller heads. In the pediatric population, the spinal cord is often included in the protocol because of the higher incidence of both primary tumors and metastases in this region. However, we have found limited clinical value of routine PET of the spinal cord and confine spine imaging to post-contrast MRI in patients without known spinal lesions. More details on the PET/MRI pediatric (and also adult) neurooncology work flow may be found in a separate publication [98].

## Conclusion

The use of combined PET and MRI is highly relevant in neurooncology and the use will increase during the years to come, whether obtained on separate or hybrid systems. Combining amino acid PET with advanced MRI shows promising results, but more research is needed to identify the most optimal use. In a clinical setting, a PET/MRI scan may increase accuracy in discriminating recurrence from treatment changes, although sequential same-day imaging on separate systems will in most situations constitute a

reliable and cost-effective alternative to hybrid PET/MRI. In pediatric patients, however, the stress of two separate examinations is significant, especially when sedation or general anesthesia is required, and this patient group will benefit most from simultaneous PET and MR imaging. Also in clinical trials, a combined PET/MRI examination may aid recruitment, standardize imaging and reduce the number of scanning procedures.

There are still a number of caveats in using a PET/MRI scanner, but solutions to overcome the challenges are being developed. Next-generation PET/MRI scanners will hopefully improve patient comfort and realize the full one-stop-shop potential of hybrid PET/MRI in neurooncology.

**Acknowledgements** The scanner assistance of technologists Karin Stahr and Marianne Federspiel and of radiographer Jákup Martin Poulsen is highly appreciated. We thank co-workers and collaborators for their kind contributions to the figures: Claes Nøhr Ladefoged (Fig. 6), Andreas Ellegaard and Jakob Slipsager (Fig. 7); Annika Langkilde for analysis of DTI data (Fig. 3); and Professor Henrik B Larsson for his kind support with the DCE method implementation (Fig. 2). The Siemens mMR hybrid PET/MR system at Copenhagen University Hospital Rigshospitalet was donated by the John and Birthe Meyer Foundation. The Child Cancer Foundation in Denmark is thanked for their generous support.

## Compliance with ethical standards

**Conflict of interest** All authors (ML, OMH, MLJ, VAL and IL) declare no conflicts of interest.

For imaging obtained in brain imaging trials, all procedures followed were in accordance with the ethical standards of the responsible committee on human experimentation (institutional and national) and with the Helsinki Declaration of 1975, as revised in 2008. Informed consent was obtained from all patients for being included in each study.

## References

1. Okada H, Weller M, Huang R, Finocchiaro G, Gilbert MR, Wick W et al (2015) Immunotherapy response assessment in neuro-oncology: a report of the RANO working group. *Lancet Oncol* 16:e534–e542
2. Wen PY, Macdonald DR, Reardon DA, Cloughesy TF, Sorensen AG, Galanis E et al (2010) Updated response assessment criteria for high-grade gliomas: response assessment in neuro-oncology working group. *J Clin Oncol* 28:1963–1972
3. Rachinger W, Goetz C, Popperl G, Gildehaus FJ, Kreth FW, Holtmannspotter M et al (2005) Positron emission tomography with O-(2-[18F]fluoroethyl)-L-tyrosine versus magnetic resonance imaging in the diagnosis of recurrent gliomas. *Neurosurgery* 57:505–511
4. Jansen NL, Graute V, Armbruster L, Suchorska B, Lutz J, Eigenbrod S et al (2012) MRI-suspected low-grade glioma: is there a need to perform dynamic FET PET? *Eur J Nucl Med Mol Imaging* 39:1021–1029
5. Kunz M, Thon N, Eigenbrod S, Hartmann C, Egensperger R, Herms J et al (2011) Hot spots in dynamic (18)FET-PET delineate malignant tumor parts within suspected WHO grade II gliomas. *Neuro Oncol* 13:307–316

6. Ellingson BM, Bendszus M, Sorensen AG, Pope WB (2014) Emerging techniques and technologies in brain tumor imaging. *Neuro Oncol* 16(Suppl 7):vii12–vii23
7. Galldiks N, Langen KJ, Pope WB (2015) From the clinician's point of view: what is the status quo of positron emission tomography in patients with brain tumors? *Neuro Oncol* 17:1434–1444
8. Albert NL, Weller M, Suchorska B, Galldiks N, Soffietti R, Kim MM et al (2016) Response Assessment in Neuro-Oncology working group and European Association for Neuro-Oncology recommendations for the clinical use of PET imaging in gliomas. *Neuro Oncol*
9. Schlemmer HP, Pichler BJ, Schmand M, Burbar Z, Michel C, Ladebeck R et al (2008) Simultaneous MR/PET imaging of the human brain: feasibility study. *Radiology* 248:1028–1035
10. Fink JR, Muzi M, Peck M, Krohn KA (2015) Multimodality brain tumor imaging: MR imaging, PET, and PET/MR imaging. *J Nucl Med* 56:1554–1561
11. Catana C, Drzezga A, Heiss WD, Rosen BR (2012) PET/MRI for neurologic applications. *J Nucl Med* 53:1916–1925
12. Werner P, Barthel H, Drzezga A, Sabri O (2015) Current status and future role of brain PET/MRI in clinical and research settings. *Eur J Nucl Med Mol Imaging* 42:512–526
13. Buchbender C, Heusner TA, Lauenstein TC, Bockisch A, Antoch G (2012) Oncologic PET/MRI, part I: tumors of the brain, head and neck, chest, abdomen, and pelvis. *J Nucl Med* 53:928–938
14. Filss CP, Galldiks N, Stoffels G, Sabel M, Wittsack HJ, Turowski B et al (2014) Comparison of 18F-FET PET and perfusion-weighted MR imaging: a PET/MR imaging hybrid study in patients with brain tumors. *J Nucl Med* 55:540–545
15. Jena A, Taneja S, Gambhir A, Mishra AK, D'souza MM, Verma SM et al (2016) Glioma recurrence versus radiation necrosis: single-session multiparametric approach using simultaneous O-(2-<sup>18</sup>F-Fluoroethyl)-L-tyrosine PET/MRI. *Clin Nucl Med*
16. Henriksen OM, Larsen VA, Muhic A, Hansen AE, Larsson HB, Poulsen HS et al (2016) Simultaneous evaluation of brain tumour metabolism, structure and blood volume using [(18F)-fluoroethyltyrosine (FET) PET/MRI: feasibility, agreement and initial experience. *Eur J Nucl Med Mol Imaging* 43:103–112
17. Bisdas S, Ritz R, Bender B, Braun C, Pfannenberg C, Reimold M et al (2013) Metabolic mapping of gliomas using hybrid MR-PET imaging: feasibility of the method and spatial distribution of metabolic changes. *Invest Radiol* 48:295–301
18. Weber WA, Wester HJ, Grosu AL, Herz M, Dzewas B, Feldmann HJ et al (2000) O-(2-<sup>18</sup>F)fluoroethyl)-L-tyrosine and L-[methyl-<sup>11</sup>C]methionine uptake in brain tumours: initial results of a comparative study. *Eur J Nucl Med* 27:542–549
19. Becherer A, Karanikas G, Szabo M, Zetting G, Asenbaum S, Marosi C et al (2003) Brain tumour imaging with PET: a comparison between [<sup>18</sup>F]fluorodopa and [<sup>11</sup>C]methionine. *Eur J Nucl Med Mol Imaging* 30:1561–1567
20. Langen KJ, Jarosch M, Muhlensiepen H, Hamacher K, Broer S, Jansen P et al (2003) Comparison of fluorotyrosines and methionine uptake in F98 rat gliomas. *Nucl Med Biol* 30:501–508
21. Grosu AL, Astner ST, Riedel E, Nieder C, Wiedenmann N, Heinemann F et al (2011) An interindividual comparison of O-(2-<sup>18</sup>F)fluoroethyl)-L-tyrosine (FET)- and L-[methyl-<sup>11</sup>C]methionine (MET)-PET in patients with brain gliomas and metastases. *Int J Radiat Oncol Biol Phys* 81:1049–1058
22. Kratochwil C, Combs SE, Leotta K, Afshar-Oromieh A, Rieken S, Debus J et al (2014) Intra-individual comparison of (1)(8)F-FET and (1)(8)F-DOPA in PET imaging of recurrent brain tumors. *Neuro Oncol* 16:434–440
23. Lapa C, Linsenmann T, Monoranu CM, Samnick S, Buck AK, Bluemel C et al (2014) Comparison of the amino acid tracers <sup>18</sup>F-FET and <sup>18</sup>F-DOPA in high-grade glioma patients. *J Nucl Med* 55:1611–1616
24. Kracht LW, Miletic H, Busch S, Jacobs AH, Voges J, Hoevels M et al (2004) Delineation of brain tumor extent with [<sup>11</sup>C]-methionine positron emission tomography: local comparison with stereotactic histopathology. *Clin Cancer Res* 10:7163–7170
25. Pauleit D, Floeth F, Hamacher K, Riemenschneider MJ, Reifenberger G, Muller HW et al (2005) O-(2-<sup>18</sup>F)fluoroethyl)-L-tyrosine PET combined with MRI improves the diagnostic assessment of cerebral gliomas. *Brain* 128:678–687
26. Ellingson BM, Bendszus M, Boxerman J, Barboriak D, Erickson BJ, Smits M et al (2015) Consensus recommendations for a standardized Brain Tumor Imaging Protocol in clinical trials. *Neuro Oncol* 17:1188–1198
27. Galldiks N, Stoffels G, Filss C, Rapp M, Blau T, Tscherpel C et al (2015) The use of dynamic O-(2-<sup>18</sup>F-fluoroethyl)-L-tyrosine PET in the diagnosis of patients with progressive and recurrent glioma. *Neuro Oncol* 17:1293–1300
28. Mehrkens JH, Popperl G, Rachinger W, Herms J, Seelos K, Tatsch K et al (2008) The positive predictive value of O-(2-<sup>18</sup>F)fluoroethyl)-L-tyrosine (FET) PET in the diagnosis of a glioma recurrence after multimodal treatment. *J Neurooncol* 88:27–35
29. Popperl G, Gotz C, Rachinger W, Gildehaus FJ, Tonn JC, Tatsch K (2004) Value of O-(2-<sup>18</sup>F)fluoroethyl)-L-tyrosine PET for the diagnosis of recurrent glioma. *Eur J Nucl Med Mol Imaging* 31:1464–1470
30. Jeong SY, Lim SM (2012) Comparison of 3'-deoxy-3'-[<sup>18</sup>F]fluorothymidine PET and O-(2-<sup>18</sup>F)fluoroethyl)-L-tyrosine PET in patients with newly diagnosed glioma. *Nucl Med Biol* 39:977–981
31. Lin NU, Lee EQ, Aoyama H, Barani IJ, Barboriak DP, Baumert BG et al (2015) Response assessment criteria for brain metastases: proposal from the RANO group. *Lancet Oncol* 16:e270–e278
32. Ellingson BM, Kim HJ, Woodworth DC, Pope WB, Cloughesy JN, Harris RJ et al (2014) Recurrent glioblastoma treated with bevacizumab: contrast-enhanced T1-weighted subtraction maps improve tumor delineation and aid prediction of survival in a multicenter clinical trial. *Radiology* 271:200–210
33. Schmainda KM (2012) Diffusion-weighted MRI as a biomarker for treatment response in glioma. *CNS Oncol* 1:169–180
34. Moffat BA, Chenevert TL, Lawrence TS, Meyer CR, Johnson TD, Dong Q et al (2005) Functional diffusion map: a noninvasive MRI biomarker for early stratification of clinical brain tumor response. *Proc Natl Acad Sci USA* 102:5524–5529
35. Ellingson BM, Cloughesy TF, Lai A, Mischel PS, Nghiemphu PL, Lalezari S et al (2011) Graded functional diffusion map-defined characteristics of apparent diffusion coefficients predict overall survival in recurrent glioblastoma treated with bevacizumab. *Neuro Oncol* 13:1151–1161
36. Pope WB, Kim HJ, Huo J, Alger J, Brown MS, Gjertson D et al (2009) Recurrent glioblastoma multiforme: ADC histogram analysis predicts response to bevacizumab treatment. *Radiology* 252:182–189
37. Kan P, Liu JK, Hedlund G, Brockmeyer DL, Walker ML, Kestle JR (2006) The role of diffusion-weighted magnetic resonance imaging in pediatric brain tumors. *Childs Nerv Syst* 22:1435–1439
38. Hilario A, Ramos A, Perez-Nunez A, Salvador E, Millan JM, Lagares A et al (2012) The added value of apparent diffusion coefficient to cerebral blood volume in the preoperative grading of diffuse gliomas. *AJNR Am J Neuroradiol* 33:701–707
39. Server A, Graff BA, Josefsen R, Orheim TE, Schellhorn T, Nordhoy W et al (2014) Analysis of diffusion tensor imaging metrics for gliomas grading at 3 T. *Eur J Radiol* 83:e156–e165

40. Potgieser AR, Wagemakers M, van Hulzen AL, de Jong BM, Hoving EW, Groen RJ (2014) The role of diffusion tensor imaging in brain tumor surgery: a review of the literature. *Clin Neurol Neurosurg* 124:51–58
41. Porter DA, Heidemann RM (2009) High resolution diffusion-weighted imaging using readout-segmented echo-planar imaging, parallel imaging and a two-dimensional navigator-based reacquisition. *Magn Reson Med* 62:468–475
42. Law M, Yang S, Wang H, Babb JS, Johnson G, Cha S et al (2003) Glioma grading: sensitivity, specificity, and predictive values of perfusion MR imaging and proton MR spectroscopic imaging compared with conventional MR imaging. *AJNR Am J Neuroradiol* 24:1989–1998
43. Fatterpekar GM, Galheigo D, Narayana A, Johnson G, Knopp E (2012) Treatment-related change versus tumor recurrence in high-grade gliomas: a diagnostic conundrum—use of dynamic susceptibility contrast-enhanced (DSC) perfusion MRI. *AJR Am J Roentgenol* 198:19–26
44. Usinskiene J, Ulyte A, Bjornerud A, Venius J, Katsaros VK, Rynkeviciene R et al (2016) Optimal differentiation of high- and low-grade glioma and metastasis: a meta-analysis of perfusion, diffusion, and spectroscopy metrics. *Neuroradiology* 58:339–350
45. Patel P, Baradaran H, Delgado D, Askin G, Christos P, Tsiouris AJ et al (2016) MR perfusion-weighted imaging in the evaluation of high-grade gliomas after treatment: a systematic review and meta-analysis. *Neuro Oncol*
46. Welker K, Boxerman J, Kalnin A, Kaufmann T, Shiroishi M, Wintermark M (2015) ASFNR recommendations for clinical performance of MR dynamic susceptibility contrast perfusion imaging of the brain. *AJNR Am J Neuroradiol* 36:E41–E51
47. Hu LS, Kelm Z, Korfiatis P, Dueck AC, Elrod C, Ellingson BM et al (2015) Impact of software modeling on the accuracy of perfusion MRI in Glioma. *AJNR Am J Neuroradiol* 36:2242–2249
48. Larsson HB, Courivaud F, Rostrup E, Hansen AE (2009) Measurement of brain perfusion, blood volume, and blood-brain barrier permeability, using dynamic contrast-enhanced T(1)-weighted MRI at 3 tesla. *Magn Reson Med* 62:1270–1281
49. Herminghaus S, Pilatus U, Moller-Hartmann W, Raab P, Lanfermann H, Schlote W et al (2002) Increased choline levels coincide with enhanced proliferative activity of human neuroepithelial brain tumors. *NMR Biomed* 15:385–392
50. McKnight TR, von dem Bussche MH, Vigneron DB, Lu Y, Berger MS, McDermott MW et al (2002) Histopathological validation of a three-dimensional magnetic resonance spectroscopy index as a predictor of tumor presence. *J Neurosurg* 97:794–802
51. Fink JR, Carr RB, Matsusue E, Iyer RS, Rockhill JK, Haynor DR et al (2012) Comparison of 3 Tesla proton MR spectroscopy, MR perfusion and MR diffusion for distinguishing glioma recurrence from posttreatment effects. *J Magn Reson Imaging* 35:56–63
52. Panigrahy A, Nelson MD Jr, Bluml S (2010) Magnetic resonance spectroscopy in pediatric neuroradiology: clinical and research applications. *Pediatr Radiol* 40:3–30
53. Gill SK, Wilson M, Davies NP, MacPherson L, English M, Arvanitis TN et al (2014) Diagnosing relapse in children's brain tumors using metabolite profiles. *Neuro Oncol* 16:156–164
54. Oz G, Alger JR, Barker PB, Bartha R, Bizzi A, Boesch C et al (2014) Clinical proton MR spectroscopy in central nervous system disorders. *Radiology* 270:658–679
55. Wang Q, Zhang H, Zhang J, Wu C, Zhu W, Li F et al (2016) The diagnostic performance of magnetic resonance spectroscopy in differentiating high-from low-grade gliomas: A systematic review and meta-analysis. *Eur Radiol* 26:2670–2684
56. Zhang H, Ma L, Wang Q, Zheng X, Wu C, Xu BN (2014) Role of magnetic resonance spectroscopy for the differentiation of recurrent glioma from radiation necrosis: a systematic review and meta-analysis. *Eur J Radiol* 83:2181–2189
57. Dickson JC, O'Meara C, Barnes A (2014) A comparison of CT- and MR-based attenuation correction in neurological PET. *Eur J Nucl Med Mol Imaging* 41:1176–1189
58. Andersen FL, Ladefoged CN, Beyer T, Keller SH, Hansen AE, Hojgaard L et al (2014) Combined PET/MR imaging in neurology: MR-based attenuation correction implies a strong spatial bias when ignoring bone. *Neuroimage* 84:206–216
59. Izquierdo-Garcia D, Hansen AE, Forster S, Benoit D, Schachoff S, Furst S et al (2014) An SPM8-based approach for attenuation correction combining segmentation and nonrigid template formation: application to simultaneous PET/MR brain imaging. *J Nucl Med* 55:1825–1830
60. Burgos N, Cardoso MJ, Thielemans K, Modat M, Dickson J, Schott JM et al (2015) Multi-contrast attenuation map synthesis for PET/MR scanners: assessment on FDG and Flortetapir PET tracers. *Eur J Nucl Med Mol Imaging* 42:1447–1458
61. Langen KJ, Bartenstein P, Boecker H, Brust P, Coenen HH, Drzezga A et al (2011) German guidelines for brain tumour imaging by PET and SPECT using labelled amino acids. *Nuklearmedizin* 50:167–173
62. Ladefoged CN, Benoit D, Law I, Holm S, Kjaer A, Hojgaard L et al (2015) Region specific optimization of continuous linear attenuation coefficients based on UTE (RESOLUTE): application to PET/MR brain imaging. *Phys Med Biol* 60:8047–8065
63. Ladefoged CN, Law I, Hassings C, Kjaer A, Hojgaard L, Andersen FL (2016) Application of the MR-AC method RESOLUTE to oncology patients with skull surgery, PSMR
64. Buther F, Vrachimis A, Becker A, Stegger L (2016) Impact of MR-safe headphones on PET attenuation in combined PET/MRI scans. *EJNMMI Res* 6:20
65. Olesen OV, Paulsen RR, Hojgaard L, Roed B, Larsen R (2012) Motion tracking for medical imaging: a nonvisible structured light tracking approach. *IEEE Trans Med Imaging* 31:79–87
66. Olesen OV, Wilm J, Van der Kouwe A, Jensen RR, Wald L (2014) An MRI Compatible Surface Scanner; Joint Annual Meeting ISMRM-ESMRMB and SMRT 1303
67. Sadeghi N, Salmon I, Tang BN, Denolin V, Levivier M, Wikler D et al (2006) Correlation between dynamic susceptibility contrast perfusion MRI and methionine metabolism in brain gliomas: preliminary results. *J Magn Reson Imaging* 24:989–994
68. Dandois V, Rommel D, Renard L, Jamart J, Cosnard G (2010) Substitution of <sup>11</sup>C-methionine PET by perfusion MRI during the follow-up of treated high-grade gliomas: preliminary results in clinical practice. *J Neuroradiol* 37:89–97
69. Sadeghi N, Salmon I, Decaestecker C, Levivier M, Metens T, Wikler D et al (2007) Stereotactic comparison among cerebral blood volume, methionine uptake, and histopathology in brain glioma. *AJNR Am J Neuroradiol* 28:455–461
70. Tietze A, Boldsen JK, Mouridsen K, Ribe L, Dyve S, Cortnum S et al (2015) Spatial distribution of malignant tissue in gliomas: correlations of <sup>11</sup>C-L-methionine positron emission tomography and perfusion- and diffusion-weighted magnetic resonance imaging. *Acta Radiol* 56:1135–1144
71. Cicone F, Filss CP, Minniti G, Rossi-Espagnet C, Papa A, Scaringi C et al (2015) Volumetric assessment of recurrent or progressive gliomas: comparison between F-DOPA PET and perfusion-weighted MRI. *Eur J Nucl Med Mol Imaging* 42:905–915
72. Kim YH, Oh SW, Lim YJ, Park CK, Lee SH, Kang KW et al (2010) Differentiating radiation necrosis from tumor recurrence in high-grade gliomas: assessing the efficacy of 18F-FDG PET, <sup>11</sup>C-methionine PET and perfusion MRI. *Clin Neurol Neurosurg* 112:758–765
73. Morana G, Piccardo A, Puntoni M, Nozza P, Cama A, Raso A et al (2015) Diagnostic and prognostic value of 18F-DOPA PET

- and 1H-MR spectroscopy in pediatric supratentorial infiltrative gliomas: a comparative study. *Neuro Oncol* 17:1637–1647
74. Floeth FW, Pauleit D, Wittsack HJ, Langen KJ, Reifemberger G, Hamacher K et al (2005) Multimodal metabolic imaging of cerebral gliomas: positron emission tomography with [<sup>18</sup>F]fluoroethyl-L-tyrosine and magnetic resonance spectroscopy. *J Neurosurg* 102:318–327
  75. Widhalm G, Krssak M, Minchev G, Wohrer A, Traub-Weidinger T, Czech T et al (2011) Value of 1H-magnetic resonance spectroscopy chemical shift imaging for detection of anaplastic foci in diffusely infiltrating gliomas with non-significant contrast-enhancement. *J Neurol Neurosurg Psychiatry* 82:512–520
  76. Nakajima T, Kumabe T, Kanamori M, Saito R, Tashiro M, Watanabe M et al (2009) Differential diagnosis between radiation necrosis and glioma progression using sequential proton magnetic resonance spectroscopy and methionine positron emission tomography. *Neurol Med Chir (Tokyo)* 49:394–401
  77. Berntsson SG, Falk A, Savitcheva I, Godau A, Zetterling M, Hesselager G et al (2013) Perfusion and diffusion MRI combined with (1)(1)C-methionine PET in the preoperative evaluation of suspected adult low-grade gliomas. *J Neurooncol* 114:241–249
  78. Karavaeva E, Harris RJ, Leu K, Shabihkhani M, Yong WH, Pope WB et al (2015) Relationship between [<sup>18</sup>F]FDOPA PET uptake, apparent diffusion coefficient (ADC), and proliferation rate in recurrent malignant Gliomas. *Mol Imaging Biol* 17:434–442
  79. Dunet V, Maeder P, Nicod-Lalonde M, Lhermitte B, Pollo C, Bloch J et al (2014) Combination of MRI and dynamic FET PET for initial glioma grading. *Nuklearmedizin* 53:155–161
  80. Rahm V, Boxheimer L, Bruehlmeier M, Berberat J, Nitzsche EU, Remonda L et al (2014) Focal changes in diffusivity on apparent diffusion coefficient MR imaging and amino acid uptake on PET do not colocalize in nonenhancing low-grade gliomas. *J Nucl Med* 55:546–550
  81. Rose S, Fay M, Thomas P, Bourgeat P, Dowson N, Salvado O et al (2013) Correlation of MRI-derived apparent diffusion coefficients in newly diagnosed gliomas with [<sup>18</sup>F]-fluoro-L-dopa PET: what are we really measuring with minimum ADC? *AJNR Am J Neuroradiol* 34:758–764
  82. Choi H, Paeng JC, Cheon GJ, Park CK, Choi SH, Min HS et al (2014) Correlation of <sup>11</sup>C-methionine PET and diffusion-weighted MRI: is there a complementary diagnostic role for gliomas? *Nucl Med Commun* 35:720–726
  83. Yoon JH, Kim JH, Kang WJ, Sohn CH, Choi SH, Yun TJ et al (2014) Grading of cerebral glioma with multiparametric MR imaging and <sup>18</sup>F-FDG-PET: concordance and accuracy. *Eur Radiol* 24:380–389
  84. D'souza MM, Sharma R, Jaimini A, Panwar P, Saw S, Kaur P et al (2014) <sup>11</sup>C-MET PET/CT and advanced MRI in the evaluation of tumor recurrence in high-grade gliomas. *Clin Nucl Med* 39:791–798
  85. Afshar-Oromieh A, Wolf MB, Kratochwil C, Giesel FL, Combs SE, Dimitrakopoulou-Strauss A et al (2015) Comparison of (6)(8)Ga-DOTATOC-PET/CT and PET/MRI hybrid systems in patients with cranial meningioma: Initial results. *Neuro Oncol* 17:312–319
  86. Thorwarth D, Henke G, Muller AC, Reimold M, Beyer T, Boss A et al (2011) Simultaneous <sup>68</sup> Ga-DOTATOC-PET/MRI for IMRT treatment planning for meningioma: first experience. *Int J Radiat Oncol Biol Phys* 81:277–283
  87. Stupp R, Mason WP, van den Bent MJ, Weller M, Fisher B, Taphoorn MJ et al (2005) Radiotherapy plus concomitant and adjuvant temozolomide for glioblastoma. *N Engl J Med* 352:987–996
  88. Kruser TJ, Mehta MP, Robins HI (2013) Pseudoprogression after glioma therapy: a comprehensive review. *Expert Rev Neurother* 13:389–403
  89. Wyss M, Hofer S, Bruehlmeier M, Hefti M, Uhlmann C, Bartschi E et al (2009) Early metabolic responses in temozolomide treated low-grade glioma patients. *J Neurooncol* 95:87–93
  90. Galldiks N, Rapp M, Stoffels G, Fink GR, Shah NJ, Coenen HH et al (2013) Response assessment of bevacizumab in patients with recurrent malignant glioma using [<sup>18</sup>F]Fluoroethyl-L-tyrosine PET in comparison to MRI. *Eur J Nucl Med Mol Imaging* 40:22–33
  91. Hutterer M, Nowosielski M, Putzer D, Waitz D, Tinkhauser G, Kostron H et al (2011) O-(2-18F-fluoroethyl)-L-tyrosine PET predicts failure of antiangiogenic treatment in patients with recurrent high-grade glioma. *J Nucl Med* 52:856–864
  92. Law I, Borjesson S, Borgwardt L, Højgaard L (2016) Pediatric hybrid imaging of the brain; Clinical molecular anatomic imaging - PET/CT. PET/MR and SPECT/CT, Wolters Kluwer Health
  93. Preuss M, Werner P, Barthel H, Nestler U, Christiansen H, Hirsch FW et al (2014) Integrated PET/MRI for planning navigated biopsies in pediatric brain tumors. *Childs Nerv Syst*
  94. Dunkl V, Cleff C, Stoffels G, Judov N, Sarikaya-Seiwert S, Law I et al (2015) The usefulness of dynamic O-(2-<sup>18</sup>F-fluoroethyl)-L-tyrosine PET in the clinical evaluation of brain tumors in children and adolescents. *J Nucl Med* 56:88–92
  95. Pirotte BJ, Lubansu A, Massager N, Wikler D, Van BP, Levivier M et al (2010) Clinical impact of integrating positron emission tomography during surgery in 85 children with brain tumors. *J Neurosurg Pediatr* 5:486–499
  96. Pirotte BJ, Lubansu A, Massager N, Wikler D, Van BP, Levivier M et al (2010) Clinical interest of integrating positron emission tomography imaging in the workup of 55 children with incidentally diagnosed brain lesions. *J Neurosurg Pediatr* 5:479–485
  97. Misch M, Guggemos A, Driever PH, Koch A, Grosse F, Steffen IG et al (2014) F-FET-PET guided surgical biopsy and resection in children and adolescence with brain tumors. *Childs Nerv Syst*
  98. Henriksen OM, Marner L, Law I (2016) Clinical PET/MR Imaging in Dementia and Neuro-Oncology. *PET Clin* 11:441–452